

Predicted properties of multiple images of the strongly lensed supernova SN Refsdal

Masamune Oguri,^{1,2,3*}

¹*Research Center for the Early Universe, University of Tokyo, 7-3-1 Hongo, Bunkyo-ku, Tokyo 113-0033, Japan*

²*Department of Physics, University of Tokyo, 7-3-1 Hongo, Bunkyo-ku, Tokyo 113-0033, Japan*

³*Kavli Institute for the Physics and Mathematics of the Universe (Kavli IPMU, WPI), University of Tokyo, Chiba 277-8583, Japan*

9 February 2015

ABSTRACT

We construct a mass model of the cluster MACS J1149.6+2223 to study the expected properties of multiple images of SN Refsdal, the first example of a gravitationally lensed supernova with resolved multiple images recently reported by Kelly et al. We find that the best-fit model predicts six supernova images in total, i.e., two extra images in addition to the observed four Einstein cross supernova images S1–S4. One extra image is predicted to have appeared about 17 years ago, whereas the other extra image is predicted to appear in about one year from the appearance of S1–S4, which is a testable prediction with near future observations. The predicted magnification factors of individual supernova images range from ~ 18 for the brightest image to ~ 4 for the faint extra images. Confronting these predictions with future observations should provide an unprecedented opportunity to improve our understanding of cluster mass distributions.

Key words: dark matter — gravitational lensing: strong — supernovae: individual: SN Refsdal

1 INTRODUCTION

The existence of strong gravitationally lensed supernovae has long been predicted (e.g., Holz 2001; Goobar et al. 2002; Oguri, Suto, & Turner 2003; Oguri & Marshall 2010). They provide a unique opportunity to study the mass distribution of lensing objects as well as cosmological parameters. For instance, the transient nature of supernovae makes it straightforward to measure arrival time differences of multiply imaged supernovae, which enables us to directly measure the absolute distance scale of the Universe (Refsdal 1964). Direct measurements of magnification factors are also possible if Type Ia supernovae are gravitationally lensed, by taking advantage of their standard candle nature. The magnification factor contains valuable information that leads to breaking degeneracies in lens potentials and cosmological parameters (Kolatt & Bartelmann 1998; Oguri & Kawano 2003; Bolton & Burles 2003).

Gravitationally lensed supernovae are predicted to be rare, which is why they have not been explored until recently. While several strongly magnified supernovae have been discovered behind massive clusters (Amanullah et al. 2011; Patel et al. 2014; Nordin et al. 2014), multiple im-

ages were not produced for these events. Quimby et al. (2013, 2014) showed that the unusual transient PS1-10afx (Chornock et al. 2013) at $z = 1.389$ was in fact a gravitationally lensed Type Ia supernova, in which PS1-10afx was shown to be magnified by a factor of 30 by a foreground lensing galaxy at $z = 1.117$. Its large magnification factor suggests that PS1-10afx must be multiply imaged (with most likely four images), which indicates that it is presumably the first discovery of a strongly lensed supernova with multiple images. However, the angular resolution of the Pan-STARRS survey was not high enough to resolve the multiple images of PS1-10afx, and hence no time delay measurement was obtained.

Recently, Kelly et al. (2015) reported the first example of *resolved* multiple images of a strongly lensed supernova from the Grism Lens-Amplified Survey from Space (GLASS; PI: T. Treu). The supernova ‘SN Refsdal’ is located in a spiral galaxy at $z = 1.491$ which itself is multiply imaged by the cluster MACS J1149.6+2223 at $z = 0.544$. Kelly et al. (2015) identified four supernova images around an elliptical cluster member galaxy, which constitute a cross-like image configuration.

In this *Letter*, we present an initial attempt to predict the property of the multiple images of SN Refsdal from a currently available lens mass model, which is crucial given the

* E-mail: masamune.oguri@ipmu.jp

timeliness of this event. We assume a flat universe with matter density $\Omega_M = 0.26$, cosmological constant $\Omega_\Lambda = 0.74$, and Hubble constant $H_0 = 72 \text{ km s}^{-1} \text{ Mpc}^{-1}$. The J2000 coordinates are used throughout the paper.

2 MASS MODELLING OF MACS J1149.6+2223

2.1 Data

The cluster MACS J1149.6+2223 was observed with the *Hubble Space Telescope* (*HST*) in several different programmes. Early *HST* observations revealed the presence of a multiply imaged face-on spiral galaxy at $z = 1.491$ (Zitrin & Broadhurst 2009; Smith et al. 2009). The cluster is also included in the ongoing Frontier Fields programme (FF; PI: Lotz). In this paper we use ‘pre-FF *HST* imaging’ data provided in the FF website¹, which were obtained in the Cluster Lensing and Supernova Survey with Hubble (CLASH; Postman et al. 2012). We select cluster member galaxies from the red-sequence in the colour-magnitude diagram with F475W and F814W band images, where galaxy magnitudes are extracted with SExtractor (Bertin & Arnouts 1996). For strong lensing constraints, we again use the same constrained used for constructing ‘pre-FF’ mass models (see, e.g., Johnson et al. 2014; Richard et al. 2014). More specifically we adopt the multiple image sets ID 1–8 and ID 13 presented in Johnson et al. (2014) for our lens mass modelling. We note that ID 9 and 10 are excluded because they are located far from the cluster centre, and ID 14 because its constraining power is weak given only two images. Spectroscopic redshifts are available only for ID 1–3; for multiple image sets with unknown source redshifts, we treat their redshifts as free parameters.

We can also take advantage of detailed morphological features of the $z = 1.491$ lensed spiral galaxy (see also Smith et al. 2009). In this paper, we identify 4 additional sub-peaks, in addition to the main core of the spiral galaxy, in the spiral arm in the *HST* image. We use the preliminary mass model constructed without including the sub-peaks to match these morphological features between different spiral galaxy images. The identified and cross-matched features are then included as observational constraints to further refine the mass model. We note that our identifications and grouping of the features are in accord with those presented in Smith et al. (2009) and Rau, Vegetti, & White (2014).

2.2 Mass Modelling

We use the public software *glafic* (Oguri 2010) to construct the mass model of MACS J1149.6+2223. In short, *glafic* adopts a parametric modelling approach in which the lens potential is described by a sum of multiple components describing dark matter haloes, cluster member galaxies, and various perturbations, and the model parameters are optimized to match observed positions of multiply imaged objects.

We describe a dark halo component by an elliptical extension of the so-called NFW (Navarro, Frenk, & White

1997) density profile. The ellipticity is introduced in the iso-density contour of the convergence. The main NFW halo is placed at the centre of the brightest cluster galaxy (BCG) at (R.A., Decl.)=(177.398749, 22.398531). In addition to the main halo, we place two additional haloes at the centres of bright cluster member galaxies at (177.392933, 22.411875) and (177.406453, 22.389575). We leave the ellipticity and position angle of the main halo at the BCG as free parameters, whereas ellipticities and position angles of the two sub-halo components are fixed to those of the observed cluster galaxies (see below). In all the halo components, the halo mass and concentration parameter are treated as free parameters.

Member galaxy components are modelled by pseudo-Jaffe ellipsoids, which contain the velocity dispersion σ and the truncation radius r_{trunc} as model parameters. In order to reduce the number of parameters, we adopt the scaling of these parameters with the galaxy luminosity in F814W band, $\sigma \propto L^{1/4}$ and $r_{\text{trunc}} \propto L^{1/2}$ (the constant mass-to-light ratio; Oguri 2010), and regard the overall normalizations of the scaling relations as free parameters. The ellipticity and position angles of individual member galaxies are fixed to values measured in the F814W image by SExtractor. To further improve the modelling accuracy we also include small perturbations of the form $\phi \propto r^2 \cos m\theta$ in the lens potential. Specifically we include $m = 2$ and 3 terms. For each term, perturbation amplitude and position angle are model parameters.

The cluster member galaxy at (177.397782, 22.395448) that produces the four Einstein cross supernova images (S1–S4) has a critical importance for fitting the supernova images. Thus we do not use the scaling relation mentioned above for this particular galaxy. Instead we place a separate pseudo-Jaffe ellipsoid with all the parameters (σ , r_{trunc} , ellipticity, and position angle) as free parameters. We use the positions of identified multiple images as observational constraints. We follow the standard mass modelling procedure to adopt positional errors larger than measurement errors considering effects of complexities of mass distributions such as asymmetry and substructures which are not fully taken into account in our parametric mass modelling. For most multiple images we adopt the positional uncertainty (in the image plane) of $\sigma = 0''.4$ which is a typical accuracy of recent cluster mass modelling (e.g., Ishigaki et al. 2015) and is also supported by the χ^2 value of our best-fitting model as we will see below. Since the lensed spiral galaxy is the host galaxy of the lensed supernova, we require slightly better accuracy of $0''.2$ for the main core and the 4 sub-peak images of the spiral galaxy. Finally we also include the observed positions of the lensed supernova (Kelly et al. 2015), which were also derived using the world coordinate system of the pre-FF *HST* imaging data, assuming even better positional uncertainty of $0''.05$ as the accurate reproduction of supernova image positions is important for the accurate prediction of time delays. In total 46 images from 14 sources are used for mass modelling. On the other hand we have 52 model parameters, indicating that the number of the degree of freedom of χ^2 fitting is 40.

¹ <http://archive.stsci.edu/prepds/frontier/lensmodels/>

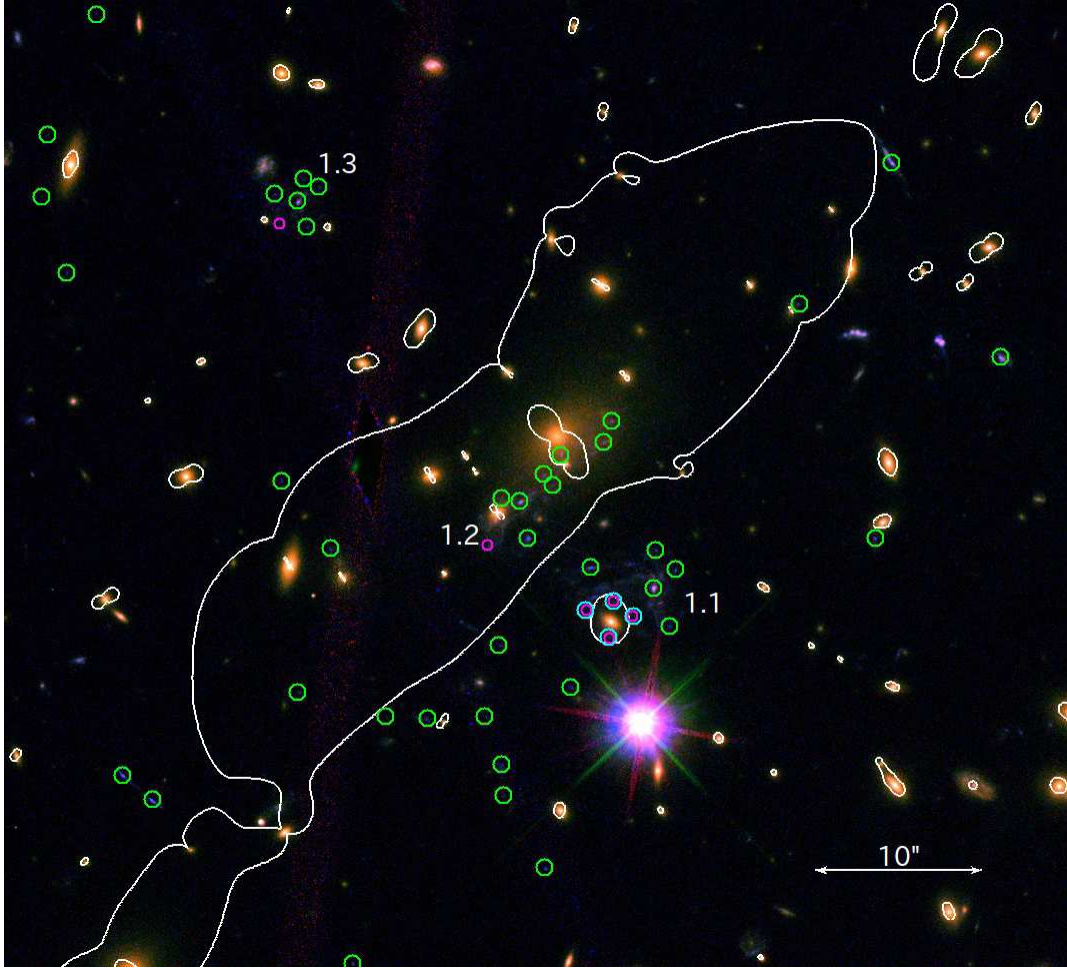


Figure 1. The colour-composite image of MACS J1149.6+2223 from the *HST* F475W-, F814W-, and F850LP-band images. The solid curve shows critical curves at $z = 1.491$ predicted by our best-fit model. North is up and West is left. Circles indicate observed multiple images (galaxy images with green circles and supernova images with cyan circles) that are used for mass modelling. The regions marked by '1.1', '1.2', and '1.3' are the locations of multiple images of a face-on spiral galaxy at $z = 1.491$, in which SN Refsdal exploded. Predicted positions of six multiple images of SN Refsdal are marked by small magenta circles.

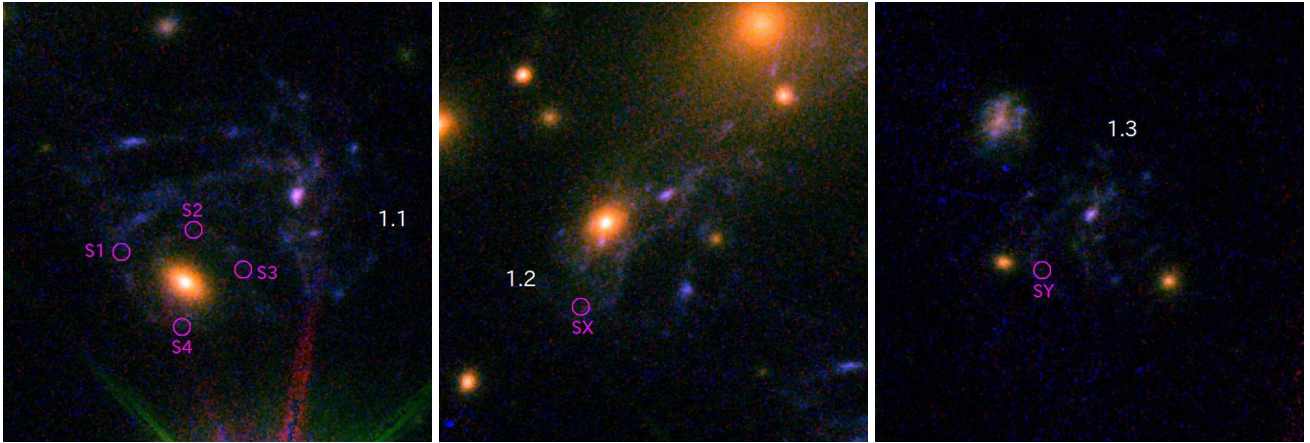


Figure 2. Zoomed images of the regions 1.1, 1.2, and 1.3 (see Figure 1). Circles show the positions of six multiple images of SN Refsdal as predicted by our best-fit model. The properties are summarized in Table 1.

Table 1. The properties of multiple images of SN Refsdal predicted by our best-fit model. μ denote the magnification factor, and Δt the time delay relative to S1.

component	R.A.	Decl.	μ	Δt [days]
S1	177.398224	22.395641	15.30	0.0
S2	177.397721	22.395782	17.66	9.2
S3	177.397383	22.395529	18.29	5.2
S4	177.397799	22.395163	8.78	22.5
SX	177.399998	22.396723	3.94	357.1
SY	177.403749	22.402076	3.78	−6193.5

3 RESULT

Our best-fit model produces $\chi^2 = 45$ for 40 degree of freedom, indicating that image positions predicted by the best-fit model agree with the observed positions with the root-mean-square value roughly equal to the input positional uncertainties, suggesting that the model reproduces multiple images almost with input positional uncertainties. Figure 1 shows the critical curves at the redshift of the supernova, $z = 1.491$, predicted by our best-fit mass model. Our best-fit model predicts six supernova images; in addition to the four Einstein cross images S1–S4 (the region 1.1 in Figure 1) which was identified by Kelly et al. (2015), there is one extra image in the region 1.2, and yet another extra image in the region 1.3. The predicted properties of the six supernova images are summarized in Table 1.

Our best-fit model predicts the high-magnifications of $\mu \sim 15 - 18$ for S1–S3, whereas the lower magnification of $\mu \sim 9$ for S4. The time delay between S1–S4 are generally short. Time delays between S1, S2, and S3 are all within 10 days, and the longest time delay between any pairs of S1–S4 are the delay between S1 and S4, 22.5 days. These predictions are consistent with the current observational data (Kelly et al. 2015).

An intriguing fact, which was also noted in Kelly et al. (2015), is the predicted presence of additional multiple images. We show the predicted positions of all the six images in Figure 2. SY is predicted to have appeared about 17 years ago, and hence there is probably no chance of detecting this image in archival images, unless the current time delay is over-predicted by a large amount. On the other hand, the image SX in the region 1.2 will appear in about one year, and therefore this prediction can be tested in near future. We however note that the deep observations are required to detect SX as the predicted magnification is smaller than that of S4.

4 SUMMARY

In this paper we have constructed a mass model of MACS J1149.6+2223 to predict the properties of multiple images of the recently discovered strongly lensed supernova RN Refsdal at $z = 1.491$ (Kelly et al. 2015). The current data already provide reasonably good constraints on the mass distribution of the core of the cluster. Our best-fit mass model predicts that there are two additional images $\sim 10''$ and $30''$ away from the four Einstein cross images S1–S4 reported by Kelly et al. (2015). One image is predicted to have appeared about 17 years ago, whereas the other image will appear 1

year after the appearance of S1–S4. The best-fit magnifications are ~ 15 for S1–S3, ~ 9 for S4, and ~ 4 for the two extra images. These results should provide useful basis of the follow-up strategy of this unique transient event.

We note that the prediction is sensitive to the mass distribution of the cluster (see also Sharon & Johnson 2015, in which different time delays are predicted), which suggests the importance of improving mass models with ongoing and future observations. For instance, GLASS observations, in which SN Refsdal was discovered, will provide spectroscopic redshifts of many background galaxies behind MACS J1149.6+2223, some of which should be multiply imaged (e.g., Schmidt et al. 2014). Ongoing *Hubble* FF programmes also provide much deeper *HST* images, from which many new sets of multiple images will be discovered (e.g., Jauzac et al. 2014). These new observations can be used to refine the mass model further, leading to more robust predictions for the supernova images. On the other hand, any mismatches between predicted and observed properties (e.g., time delays) indicate the room for improvements of our understanding of cluster mass distributions.

ACKNOWLEDGMENTS

I thank R. Quimby, S. More, A. More, M. Werner, K. Nomoto for useful discussions. This work was supported in part by World Premier International Research Center Initiative (WPI Initiative), MEXT, Japan, and Grant-in-Aid for Scientific Research from the JSPS (26800093).

REFERENCES

- Amanullah R., et al., 2011, *ApJ*, 742, L7
- Bertin E., Arnouts S., 1996, *A&AS*, 117, 393
- Bolton A. S., Burles S., 2003, *ApJ*, 592, 17
- Chornock R., et al., 2013, *ApJ*, 767, 162
- Goobar A., Mörtzell E., Amanullah R., Nugent P., 2002, *A&A*, 393, 25
- Holz D. E., 2001, *ApJ*, 556, L71
- Ishigaki M., Kawamata R., Ouchi M., Oguri M., Shimasaku K., Ono Y., 2015, *ApJ*, 799, 12
- Jauzac M., et al., 2014, *MNRAS*, 443, 1549
- Johnson T. L., Sharon K., Bayliss M. B., Gladders M. D., Coe D., Ebeling H., 2014, *ApJ*, 797, 48
- Kelly P. L., et al., 2015, *arXiv:1411.6009*
- Kolatt T. S., Bartelmann M., 1998, *MNRAS*, 296, 763
- Navarro J. F., Frenk C. S., White S. D. M., 1997, *ApJ*, 490, 493
- Nordin J., et al., 2014, *MNRAS*, 440, 2742
- Oguri M., 2010, *PASJ*, 62, 1017
- Oguri M., Kawano Y., 2003, *MNRAS*, 338, L25
- Oguri M., Marshall P. J., 2010, *MNRAS*, 405, 2579
- Oguri M., Suto Y., Turner E. L., 2003, *ApJ*, 583, 584
- Patel B., et al., 2014, *ApJ*, 786, 9
- Postman M., et al., 2012, *ApJS*, 199, 25
- Quimby R. M., et al., 2013, *ApJ*, 768, L20
- Quimby R. M., et al., 2014, *Sci*, 344, 396
- Rau S., Vegetti S., White S. D. M., 2014, *MNRAS*, 443, 957
- Refsdal S., 1964, *MNRAS*, 128, 307

Richard J., et al., 2014, MNRAS, 444, 268
Schmidt K. B., et al., 2014, ApJ, 782, L36
Sharon K., Johnson T. L., 2015, arXiv, arXiv:1411.6933
Smith G. P., et al., 2009, ApJ, 707, L163
Zitrin A., Broadhurst T., 2009, ApJ, 703, L132